ELSEVIER

Energetic electron flux behavior at low L-shells and its relation to the South Atlantic Anomaly

Timo Asikainen*, Kalevi Mursula

Department of Physical Sciences, P.O. Box 3000, FIN-90014, University of Oulu, Finland

Abstract

Here we study energetic electron fluxes in the inner radiation belt ($L<2$), especially within the South Atlantic Anomaly (SAA) region during a period of a few months using data from the low-altitude NOAA-15 and 16 satellites. Observations by these two spacecraft can yield long-term measurements of energetic electron fluxes at four different local time sectors. We discuss the time development as well as local time and longitude dependence of energetic electron fluxes around the magnetic equator at $L<2$ inside and outside of the SAA region. In particular, we concentrate on the observed local time dependence of trapped and precipitating fluxes inside the SAA region and the observed interesting differences between the trapped and precipitating components. Our observations show that there is a strong and stable dawn–dusk asymmetry in the precipitating electron flux (fluxes higher in the dawn) inside the SAA present at all times. Trapped electron fluxes inside the SAA exhibit a clear local time dependence where the fluxes are maximum at night side and decrease towards east. We have suggested an explanation for these features in terms of inward radial transport of electrons mainly in the night side and wave–particle interactions that could cause the dawn–dusk asymmetry in precipitation.
© 2007 Elsevier Ltd. All rights reserved.

Keywords: Energetic electrons; South Atlantic Anomaly; Inner radiation belt; Local-time dependence

1. Introduction

The energetic electrons in the Earth's radiation belts are concentrated in two regions: the inner and outer belts. The inner belt typically resides below the distance of $2R_E$ while the outer belt is located at a distance of about 4–$8R_E$. The dynamics of radiation belt electrons has been studied extensively (see, e.g., a review by Friedel et al., 2002) and the variations in the electron fluxes have been shown to be a result of a rather complicated mixture of different processes such as radial diffusion, acceleration by ULF waves (e.g., Elkington et al., 2003) and whistler-mode waves (Horne et al., 2005) as well as pitch angle diffusion by Coulomb collisions and interaction with different plasma waves (Abel and Thorne, 1998). These different processes play a role in the dynamics of both the inner and outer radiation belt electrons although the relative contribution of different processes strongly depends on the radial distance and local time (Friedel et al., 2002; Green et al., 2005).

The radiation belt particles are also strongly affected by the presence of the South Atlantic

*Corresponding author. Tel.: +358 8 5531302;
fax: +358 8 5531303.

E-mail address: timo.asikainen@oulu.fi (T. Asikainen).
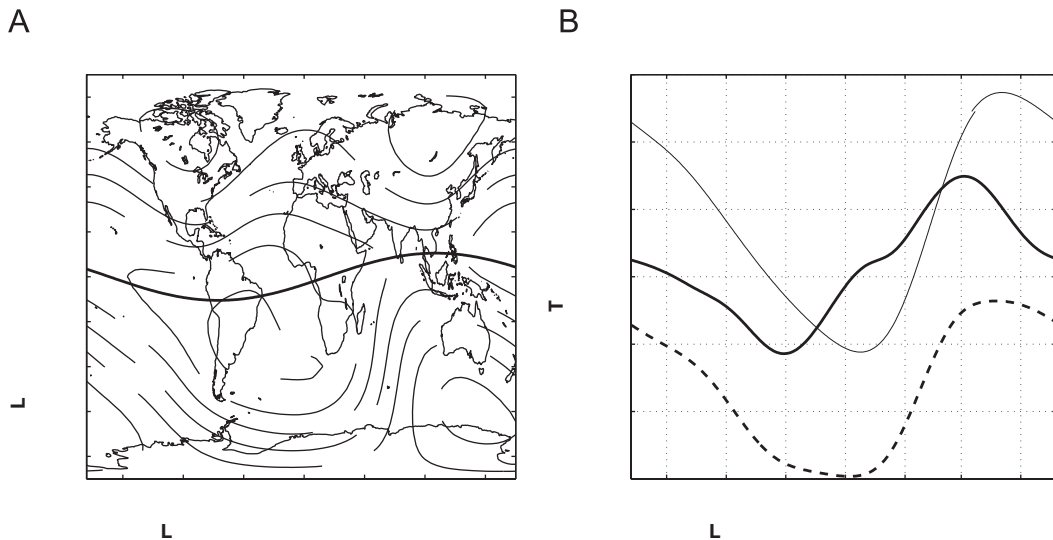
A

B

Fig. 1. (A) Magnetic field intensity at the NOAA orbit altitude (850 km) from the IGRF-2000 model (interpolated to year 2001). The thick line shows the magnetic dipole equator. (B) Magnetic field intensity at NOAA altitude as a function of geographic longitude for $L = 1:13$ (thick), $L = 1:3$ (thin) and $L = 1:58$ (dashed).

Anomaly (SAA), which is a region of decreased magnetic field over the Southern Atlantic ocean and South America (see Fig. 1) (Pinto et al., 1992). The region arises due to the offset of the Earth's dipole of about 436 km from the Earth's center towards direction of southeast Asia. The presence of SAA leads to the fact that particles drifting around the Earth in closed orbits can be quasi-trapped instead of being stably trapped or precipitating. Particles that are quasi-trapped have such pitch angles that outside the SAA they are not in the local loss cone but their pitch angle is small enough so that they precipitate when they enter the SAA region. These particles are said to be in the drift loss cone, which is the maximum local loss cone inside the SAA region. The particle precipitation and the longitudinal asymmetries in the geomagnetic field due to SAA have been studied in the past (see, e.g., Pinto and Gonzalez, 1989; Selesnick et al., 2003). However, most of the past studies have concentrated on the high energy (MeV range) electrons. In this study we concentrate on the lower energy part of the radiation belts from 30 keV to 2.5 MeV, especially on the behavior of these particles on longer time scales inside the SAA at different local times.

2. Instrumentation and data

In this work we use energetic electron data from the Medium Energy Proton Electron Detector (MEPED) instrument which is a part of the SEM-2 space environment monitoring package onboard polar orbiting NOAA-15 and NOAA-16 satellites. The altitude of the satellites is about 850 km and the orbital period about 1 h 40 min. Thus the minimum L-shell crossed by the satellites during their orbit is about $L = 1:13$. The orbital planes of NOAA-15 and NOAA-16 are 7–19 LT and 2–14 LT. We will call the 02, 07, 14 and 19 LT sectors as night, dawn, noon and dusk, respectively. Using these two NOAA satellites we can monitor energetic particle fluxes at four different LT sectors at the time resolution of one orbital period.

MEPED includes two sensors that measure particle fluxes in two independent directions, one (so-called 01 detector) roughly along the local vertical direction, the other (901 detector) perpendicular to it. At low latitudes (and L-shells) close to the magnetic equator the 01 detector measures mainly trapped particles while at high latitudes it measures the precipitating particles and vice versa for the 901 detector. The electrons are measured at three energy channels (30–100 keV, 100–300 keV and 300 keV–2.5 MeV). A more comprehensive description about the NOAA/POES satellites and their energetic particle instruments is provided by Evans and Greer (2000).

We are interested in the characteristics of the inner radiation belt ($L < 2$) electrons especially in the SAA during an extended period of time. The time

period selected for this study extends from February to May 2001. For the purpose of this study we downsampled the data by calculating average electron fluxes during half an orbit from pole to pole at $L < 2$ (McIlwain L-value) which corresponds to magnetic latitudes below about 41l. The minimum L-shell attained by the satellites during their orbit is approximately $L = 1{:}12$ and thus the data are averaged over $L \approx [1{:}12; 2]$. The average fluxes were calculated in this way separately for each of the three energy channels and two detectors. In addition, the total fluxes were calculated from these by summing the fluxes from individual channels. We also calculated the corresponding average geographic longitude and magnetic local time of the satellites. Since the observations were restricted to the equatorial region ($L < 2$) where the 01 detector measures the trapped particles and 901 detector the precipitating ones, we will from here on call the electrons at these directions as trapped and precipitating. The downsampled data allow us to study the electron fluxes at the orbital time resolution of 1 h 40 min in four local time sectors as a function of time and geographic longitude. It should be noted that the MEPED electron detectors are sensitive to protons with energy above about 210 keV. We have checked, however, that in the $L < 2$ region the electron fluxes are always much higher than the proton fluxes about 210 keV. Thus we are confident that the proton contamination does not affect the conclusions made in this paper.

3. Observations

3.1. Overview of energetic electron fluxes at the inner radiation belt

Fig. 2 displays the total trapped and precipitating electron fluxes in the energy range from 30 keV to 2.5 MeV at $L < 2$ from both NOAA-15 and 16 satellites, the Dcx (corrected Dst) index (in which the Sq-variation of the magnetic X-component is properly subtracted away, Mursula and Karinen, 2005; Karinen and Mursula, 2006) as well as solar wind speed and dynamic pressure in one panel. The trapped flux seems to follow the storm activity closely during the relatively quiet time when the Dcx4 −100 nT (from February until mid-March), returning nearly back to the quiet time level after each enhancement. During the strong storms in March–April the trapped fluxes increase by 1–2 orders of magnitude relative to the quiet time level,

and stay above it at least until the end of the studied time interval. After the rise of the electron flux level the good correlation between Dcx and trapped electron fluxes disappears. We speculate that the rise of the flux levels is most likely related to the repeated high-speed solar wind streams in the first half of April 2001.

The precipitating fluxes are quite stable up to the strong storm period in April–May when the precipitating flux levels rise nearly by an order of magnitude. However, the overall level of precipitation still stays remarkably stable in contrast to the behavior of the trapped fluxes. Note also that during the quiet time the overall ratio between trapped and precipitating fluxes is slightly less than one but during the strong storms the ratio is about two. However, the momentary maxima of trapped fluxes can be an order of magnitude larger than the precipitating fluxes.

3.2. Longitude structure

The total trapped and precipitating electron fluxes in the energy range from 30 keV to 2.5 MeV are shown in Fig. 3 as a function of geographic longitude. The longitudinal distributions are shown separately for the four local time sectors monitored by the NOAA-15 and 16. One can see considerable differences between the trapped and precipitating fluxes. The trapped fluxes are very closely concentrated between about −1001 and 401 longitude with the maximum at about −501 longitude. This maximum corresponds well to the minimum magnetic field intensity in the SAA at $L = 1{:}13$ (see Fig. 1B). Note that the longitudinal shape of the trapped flux profile does not exactly follow any given magnetic field profile in Fig. 1B since the fluxes are averaged over a range of L-values ($L = 1 - 2$). The fluxes outside the SAA region are very small but some enhancements are seen eastwards of 1501. These enhancements occur only during strong storms when Dcx < − 100 nT.

The precipitating fluxes are seen at all longitudes both inside and outside the SAA. However, the fluxes inside the SAA are roughly an order of magnitude larger than outside the SAA. The precipitation maximum seems to be concentrated around 01 longitude. Another feature which is clearly visible in the precipitating flux profile is that the fluxes inside the SAA seem to be concentrated around two bands (one of higher flux and one of lower). This band structure is a result of the sudden
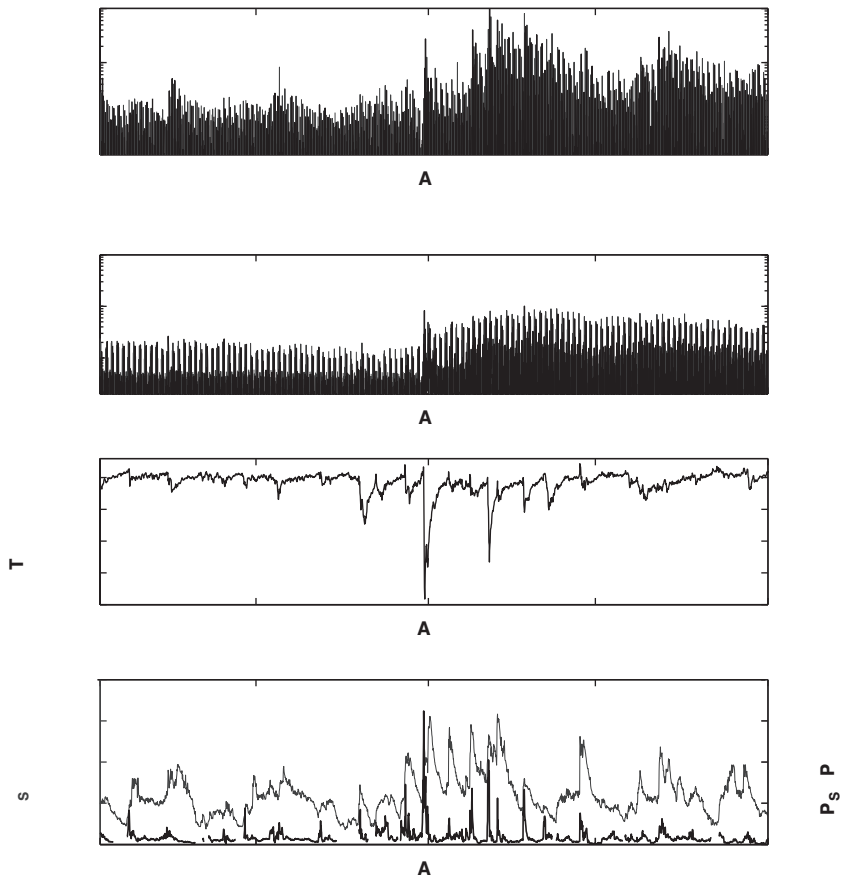
Fig. 2. Overview of inner radiation belt electron fluxes for February–May 2001. Panels from top to bottom depict total trapped electron flux (30 keV–2.5 MeV), total precipitating electron flux (30 keV–2.5 MeV), Dcx index and solar wind speed and dynamic pressure (in one panel), respectively.

increase in the overall flux level that occurred after March 31 2001, storm (see Fig. 2). In February–March the precipitating fluxes follow the lower band and in April–May the higher band. An overall increase in the trapped flux level is also seen in Fig. 2, although the trapped flux levels are much more variable than the level of precipitating fluxes. This increase of trapped flux level causes the 1–2 orders of magnitude variation in the peak trapped flux inside the SAA around −501 longitude.

3.3. Local time dependence

The top two panels of Fig. 3 show the flux profiles for night and dawn sectors while the two bottom panels show the profiles for noon and dusk sectors. The differences between the different LT sectors are most visible in the precipitating flux. The overall level of precipitation inside the SAA region seems to be about an order of magnitude larger in the night/dawn sectors than in the noon/dusk. This same feature is seen in Fig. 2 where the precipitating flux clearly shows two distinct envelopes, the upper of which corresponds to the night/dawn flux level and the lower to noon/dusk level. Outside the SAA the precipitation level in the longitude region −1801 to −1001 seems to be in the noon/dusk sectors stronger than in the night/dawn sector. The LT structure of trapped electrons is less evident in Fig. 3 but it is clear that the maximum fluxes at the night/dawn side are larger on average than the fluxes at the noon/dusk sector. Fig. 4 shows the average trapped electron fluxes as a function of longitude in linear scale. In this figure the difference between different LTs is clear: the peak flux level is highest in the night side and decreases with increasing local time.
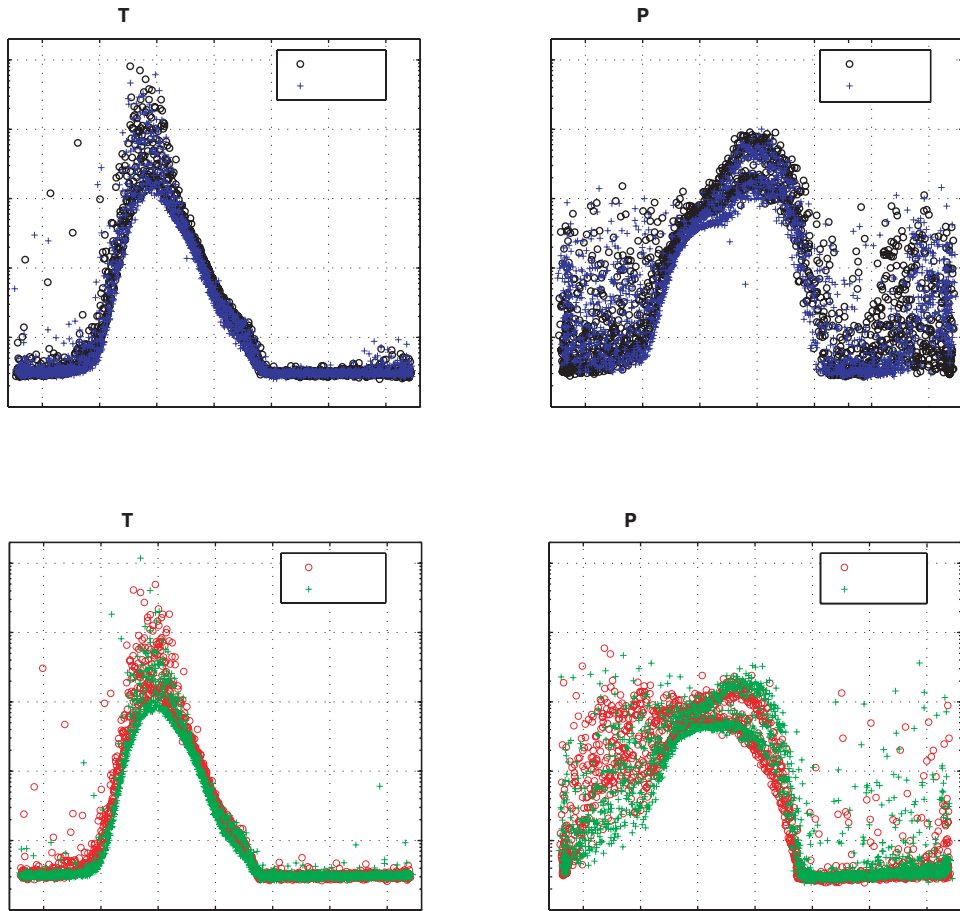
Fig. 3. Total trapped and precipitating electron fluxes (30 keV–2.5 MeV) as a function of geographic longitude for four different local time sectors.
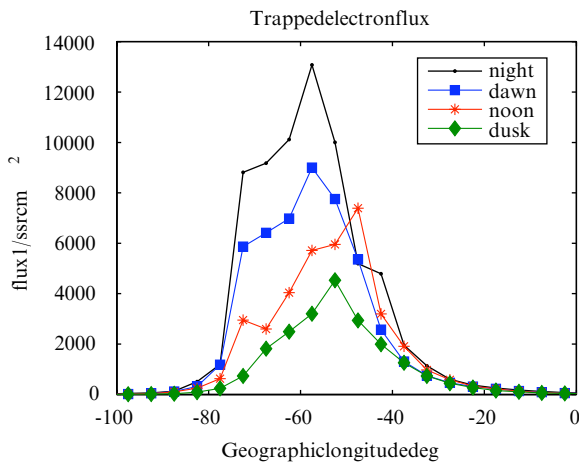

Fig. 4. Median trapped electron flux as a function of geographic longitude. The medians are calculated in 5 degree longitude bins.

However, the flux levels east of −301 longitude remain very similar at all LT sectors.

4. Discussion and conclusions

The longitude structure of electron fluxes in the inner radiation belt observed at NOAA altitude can be understood by considering the local magnetic field intensity in Fig. 1B. Trapped electrons drifting eastwards close to the magnetic equator follow the paths of constant magnetic field (constant magnetic moment). When the local magnetic field starts to decrease when approaching the SAA the electrons descend to lower altitudes in order to conserve their magnetic moment. The longitude structure of the trapped fluxes indicates that most trapped electrons drift at altitudes greater than the NOAA altitude

(850 km) outside the SAA. During active times the trapped electrons are transported to lower L-shells so that they are also occasionally observed even outside the main SAA region. However, even during storms we see very few trapped flux enhancements in the region 50–1401 (see Fig. 3 left) where the magnetic field is strongest (see Fig. 1B).

The longitude structure of precipitating electrons can also be understood in terms of the local magnetic field intensity. The fluxes are generally higher inside the SAA due to the lower magnetic field intensity. The maximum flux, however, does not correspond to the minimum magnetic field along the magnetic equator but is rather located at the eastern edge of the SAA especially at the night/dawn sector (see Fig. 3 right). The position of the maximum precipitating flux corresponds to the small 'tongue' of decreased magnetic field around -351 latitude and 01 longitude, where the magnetic field intensity minimum resides at $L \approx 1:5$. This region is at a higher L-shell than the SAA -501 longitude region, thus closer to the center of the inner radiation belt, where the electron fluxes are higher than on lower L-shells.

The precipitating fluxes seen outside the SAA can be understood as coming from those field lines whose equatorial altitude is greater than the altitude of NOAA orbit (L-shell greater than 1.13). Assuming that at these low L-shells the electron distribution peaks at 901 pitch angle the level of precipitating fluxes outside the SAA gives a lower limit to the flux of trapped electrons at altitudes higher than the NOAA altitude. As the electron populations descend to lower altitudes in the SAA the trapped electrons are also observed. Indeed, the precipitating fluxes outside the SAA are smaller than the trapped fluxes inside the SAA (the fluxes that are above the NOAA altitude outside SAA).

The local time distribution of trapped electrons (see Fig. 4) suggests that there is a real local time asymmetry in the trapped component of inner radiation belt electrons. Since the electrons drift eastwards and the trapped fluxes are greatest at the night side it seems that the electrons are mainly transported into the low altitudes at night side. It might be that when the SAA is at the night side the electrons transported into the inner radiation belt can penetrate deeper than on other longitudes. Due to the conservation of the first adiabatic invariant it would require less energy to transport a particle inward into the weaker magnetic field in SAA than into the stronger magnetic field outside the SAA. In other words, with a given energy contained in the ULF fluctuations producing the radial diffusion the electrons would be expected to be transported deeper when the field near the Earth is weaker. On the basis of this the further the SAA is eastward of the night sector the stronger is the local magnetic field at the night side (see Fig. 1, westward of SAA) and the harder it is for electrons to penetrate to same L-shells as they did inside the SAA. This interpretation is supported by trapped flux observations in Fig. 3 where the number and strength of electron injections outside the SAA is anticorrelated with the local magnetic field strength shown in Fig. 1b. The local time distribution of precipitating electrons is more difficult to understand. The precipitating fluxes are characterized by a strong asymmetry between night/dawn and noon/dusk sectors as well as remarkably stable flux levels. Most likely the precipitation inside the SAA is caused by enhanced pitch-angle diffusion into the drift loss cone by different whistler-mode wave–particle interactions in the plasmasphere which are known to exhibit strong local time asymmetries (as described by, e.g., Green et al., 2005).

References

Abel, B., Thorne, R.M., 1998. Electron scattering loss in the Earth's inner magnetosphere: 1. Dominant physical processes. Journal of Geophysical Research 103, 2385–2396.

Elkington, S.R., Hudson, M.K., Chan, A.A., 2003. Resonant acceleration and diffusion of outer zone electrons in an asymmetric geomagnetic field. Journal of Geophysical Research 108 (A3), 1116.

Evans, D.S., Greer, M.S., 2000. Polar orbiting environmental satellite space environment monitor—2: instrument descriptions and archive data documentation. NOAA Technical Memorandum, Boulder, Colorado OAR SEC-93.

Friedel, R.H.W., Reeves, G.D., Obara, T., 2002. Relativistic electron dynamics in the inner magnetosphere: a review. Journal of Atmospheric and Solar-Terrestrial Physics 64, 265–282.

Green, J.L., Boardsen, S., Garcia, L., Taylor, W.W.L., Fung, S.F., Reinisch, B.W., 2005. On the origin of whistler mode radiation in the plasmasphere. Journal of Geophysical Research 110, A03201.

Horne, R.B., Thorne, R.M., Shprits, Y.Y., et al., 2005. Wave acceleration of electrons in the Van Allen radiation belts. Nature 437, 227–230.

Karinen, A., Mursula, K., 2006. Correcting the Dst index: consequences for absolute level and correlations. Journal of Geophysical Research A 111, A08207.

Mursula, K., Karinen, A., 2005. Explaining and correcting the excessive semiannual variation in the Dst index. Geophysical Research Letters 32, L14107.

Pinto, O., Gonzalez, W.D., 1989. Energetic electron precipitation at the South Atlantic Magnetic Anomaly: a review. Journal of Atmospheric and Terrestrial Physics 51 (5), 351–365.

Pinto, O., Gonzalez, W.D., Pinto, R.C.A., Gonzalez, A.L.C., Mendes, O., 1992. The South Atlantic Magnetic Anomaly: three decades of research. Journal of Atmospheric and Terrestrial Physics 54 (9), 1129–1134.

Selesnick, R.S., Blake, J.B., Mewaldt, R.A., 2003. Atmospheric losses of radiation belt electrons. Journal of Geophysical Research 108 (A12), 1468.